Neuron, Vol. 33, 559–571, February 14, 2002, Copyright ©2002 by Cell Press

Drosophila Dscam Is Required for Divergent Segregation of Sister Branches and Suppresses Ectopic Bifurcation of Axons

Jian Wang,[1] Christopher T. Zugates,[1] Inray H. Liang,[1] Ching-Hsien J. Lee,[2] and Tzumin Lee[1,3]
[1]Department of Cell and Structural Biology
University of Illinois
Urbana, Illinois 61801
[2]Section of Hematology/Oncology
Department of Medicine
University of Illinois
Chicago, Illinois 60612

Summary

Axon bifurcation results in the formation of sister branches, and divergent segregation of the sister branches is essential for efficient innervation of multiple targets. From a genetic mosaic screen, we find that a lethal mutation in the *Drosophila* Down syndrome cell adhesion molecule (Dscam) specifically perturbs segregation of axonal branches in the mushroom bodies. Single axon analysis further reveals that *Dscam* mutant axons generate additional branches, which randomly segregate among the available targets. Moreover, when only one target remains, branching is suppressed in wild-type axons while *Dscam* mutant axons still form multiple branches at the original bifurcation point. Taken together, we conclude that Dscam controls axon branching and guidance such that a neuron can innervate multiple targets with minimal branching.

Introduction

Innervation of multiple targets by a neuron requires the formation of axonal branches. Currently, the cellular and molecular mechanisms governing axon branch formation are poorly understood (reviewed in Acebes and Ferrus, 2000). Morphological evidence indicates that axonal branches develop either as skinny collaterals from existing axons or as split processes during bifurcation of axons (Sato et al., 1994; Bastmeyer and O'Leary, 1996; Matheson and Levine, 1999). Axon bifurcation occurs when one growth cone is split into two and the two growth cones diverge. The directional segregation of the growth cones and thus the sister branches derived from a single axon are essential for propagating neural signals in divergent directions.

Many genetic and molecular studies of axon guidance indicate that cell fate plays a crucial role in determining the projection patterns of individual axons (e.g., Wang et al., 1998; Thor et al., 1999; Moran-Rivard et al., 2001; Pierani et al., 2001). The growth cones of distinct axons are differentially specialized such that distinct growth cones respond to different guidance cues and sometimes make unique responses to common signals during their journeys to intermediate/final targets (e.g., Winberg et al., 1998; Chen et al., 1998; Song et al., 1998; Hong et al., 1999; for reviews, see Tessier-Lavigne and Goodman, 1996; Song and Poo, 1999). So if axon bifurcation leads to formation of "twin" growth cones, how can these growth cones with the same cell fate faithfully project away from each other and toward different targets? This simultaneous extension and divergence of twin growth cones might be achieved simply by mutual repulsion mechanisms. Alternatively, during or soon after bifurcation, individual growth cones might further differentiate and acquire distinct sets of guidance receptors through interactions between each other or with different glial cells. Evidence suggests that the properties of growth cones are dynamically regulated during the navigation process and perhaps independently of their cell bodies (Shaw et al., 1977; Mason and Wang, 1997). For instance, recent studies on the Robo/Comm-regulated midline crossing of axons nicely demonstrate that growth cones can dynamically adjust their guidance receptors such that they only cross the midline once (Tear et al., 1996; Kidd et al., 1998, 1999). In addition, some neurons project their processes both contralaterally and ipsilaterally (Sugihara et al., 1999), supporting that individual growth cones derived from a single neuron act as independent navigating units. So sister growth cones may assume individual autonomy immediately following bifurcation, such that the growth cones derived from a single neuron can respond to different guidance cues or the same guidance cues but in different manners. The speculation surrounding differential guidance of sister growth cones reminds us that nothing is known about the underlying molecular mechanisms.

The molecular mechanisms that control the location and number of bifurcations are also poorly understood (Matheson and Levine, 1999; Wang et al., 1999; Acebes and Ferrus, 2000). It is likely that bifurcation patterns are regulated through interactions between growth cones and their local environments that result in the formation of the correct number of branches at specific sites (Gallo and Letourneau, 1998). Given that pioneer axons play critical roles in establishing the trajectories for their follower processes (Pike et al., 1992; Hidalgo and Brand, 1997), distinct mechanisms might be used to mediate branch formation in pioneer axons versus their follower processes (Fashena and Westerfield, 1999). In addition, formation of multiple branches is probably achieved by repeated bifurcation, because no more than two processes share a common origin in all documented instances of neurite arborization (Acebes and Ferrus, 2000). Since two branching events can occur as closely as 1 μm apart (Acebes and Ferrus, 2000), induction of bifurcation, suppression of multifurcation, and how quickly bifurcation can be reinduced may all be actively regulated.

Regulation of growth cone bifurcation and guidance are undoubtedly essential to the development of the *Drosophila* mushroom body (MB), the olfactory learning and memory center in insects (Heisenberg et al., 1985; de Belle and Heisenberg, 1994; Connolly et al., 1996; Grotewiel et al., 1998). In the MB neuropil, most axons

[3]Correspondence: tzumin@life.uiuc.edu

end with two major processes that project away from each other at a right angle (Strausfeld, 1976; Lee et al., 1999). The two processes extending from individual axons are morphologically indistinguishable until the neuron matures and the axonal processes acquire distinct secondary branching patterns (Lee et al., 1999). Examination of axonal morphogenesis in young MB neurons further reveals that extension of these major axonal branches is relatively synchronized (our unpublished observation). All of these observations support that bifurcation of MB axons is probably a result of growth cone splitting. Given that four neuroblasts simultaneously generate MB neurons during development (Truman and Bate, 1988; Ito and Hotta, 1992), selective fasciculation of only one branch from every neuron without error could be quite challenging. For instance, simple repulsion or competition mechanisms would not allow more than one growth cone to extend along the same path, which would make it impossible to segregate four sets of sister branches into just two fascicles simultaneously.

To facilitate mosaic analysis in the complex CNS, we have developed a novel genetic mosaic system, called MARCM, in which only the homozygous cells lacking GAL80 are uniquely labeled in mosaic tissues (Lee and Luo, 1999). Using the MARCM genetic mosaic system, we recently described the wild-type development of the *Drosophila* MB with unprecedented single-cell resolution (Lee et al., 1999). Moreover, by creating clones of MB neurons homozygous for various mutations in mosaic organisms, we started to elucidate the molecular mechanisms controlling different aspects of MB development (Lee et al., 2000a, 2000b; Scott et al., 2001; for reviews, see Lee and Luo, 2001). Interestingly, from a genetic mosaic screen designed for identifying novel mutations that cause specific defects in the development of MB neurons, we found a lethal mutation that specifically hinders the formation of bifurcated axon bundles. If the mutant clone is created before the birth of neurons that normally project two perpendicular fascicles, these neurons will instead extend their axons in only one of the two original directions. We also find that one mutant neuroblast clone in the whole MB can alter the projections of the other three wild-type clonal units. Phenotypic analysis of single neurons further reveals that mutant axons give rise to additional branches at the bifurcation point and that the branches are distributed randomly among the accessible pathways. When only one path exists, wild-type neurons project a single process along the path while mutant neurons generate multiple branches. In addition, defects in axon extension are observed in certain mutant MB neurons. Mapping by recombination and complementation reveals this interesting lethal mutation as an allele of the *Drosophila Dscam* gene (Schmucker et al., 2000), suggesting a novel molecular mechanism for mediating formation and guidance of axonal branches.

Results

Identification of a Novel *Dscam* Mutation that Disrupts Formation of the MB α and β Lobes

The MBs are paired structures, one in each brain lobe; and one MB is derived from four neuroblasts (Nbs), each of which generates a similar set of three distinct types of neurons (Ito et al., 1997; Lee et al., 1999). γ neurons, which are generated prior to the mid-3rd instar stage, project axons into the γ lobe at the adult stage; α'/β' neurons, which are generated in late 3rd instar, have bifurcated axons that form the α' and β' lobes; and α/β neurons, which are generated after puparium formation (PF), project their bifurcated axonal branches into the α and β lobes (Lee et al., 1999; Figure 1A). In an ongoing genetic mosaic screen (see Experimental Procedures), we identified a novel lethal mutation, *l(2R)MB99*, that causes various defects in the guidance of bifurcated α/β axons.

When subsets of cells within wild-type MB Nb clones are selectively marked using GAL4-201Y (Yang et al., 1995), all labeled axons extend either into the γ lobe or the α and β lobes; the α lobe extends dorsally while the γ and β lobes extend medially toward the midline (Figures 2A–2C). Only a small number of the late pupal-born α/β neurons are marked, so the α and β lobes appear very thin and faint as compared with the γ lobe (Figure 1B). In addition, these labeled axons occupy the center of the α and β lobes (Figure 2C). These GAL4-201Y-marked α and β lobes are hereafter referred to as the core α and β lobes (Yang et al., 1995). Notably, the core α and β lobes are morphologically indistinguishable (Figure 1B), consistent with the fact that individual α/β axons bifurcate into two branches that project away from each other into the α and β lobes, respectively (Lee et al., 1999). A total of 50 *l(2R)MB99* mutant Nb clones were collected for detailed phenotypic analysis. In contrast with normal looking γ lobes, abnormal α/β lobes are observed in every Nb clone homozygous for the *l(2R)MB99* mutation (Figures 1C and 1D). Being much thicker and denser than in wild-type clones, the core α/β lobes seem to be composed of many more axons in the *l(2R)MB99* mutant clones (Figure 1C, compared with Figure 1B). But, unlike wild-type α/β axons, most mutant core α/β processes appear to fail to reach the ends of the α/β lobes (Figures 1C and 1D). Because no change in the number of cell bodies can be detected (about 30 GAL4-201Y-positive α/β neurons in each Nb clone), the morphological changes observed in mutant core α/β bundles imply that individual α/β axons acquire supernumerary but short-ending branches in mutant clones. In addition, dramatic changes in the configuration of the α/β lobes are observed in 38% of mutant Nb clones (Figures 1D, 2D, and 2G). Instead of bifurcating axons at a right angle, these mutant clones project all of their α/β axons in only one direction, either dorsally or medially. Interestingly, these uni-directionally extending mutant processes can exist as two distinct bundles running side by side (Figure 2D), or can be fasciculated into a single bundle (Figures 1D and 2G). Another phenotype that suggests defects in the divergent segregation of α/β axonal branches is detected in about 20% of mutant Nb clones, where differences in the thickness of the axon bundles exist between the dorsal and medial fascicles (data not shown, similar to Figure 3G). These complicated, wide-ranging abnormalities underscore the importance of the phenotypic analysis of individual axons (see below).

In order to identify the mutation responsible for these interesting axon guidance defects, we first mapped one lethal mutation in the *l(2R)MB99* line to the 43 cytogenetic locus by recombination (see Experimental Proce-

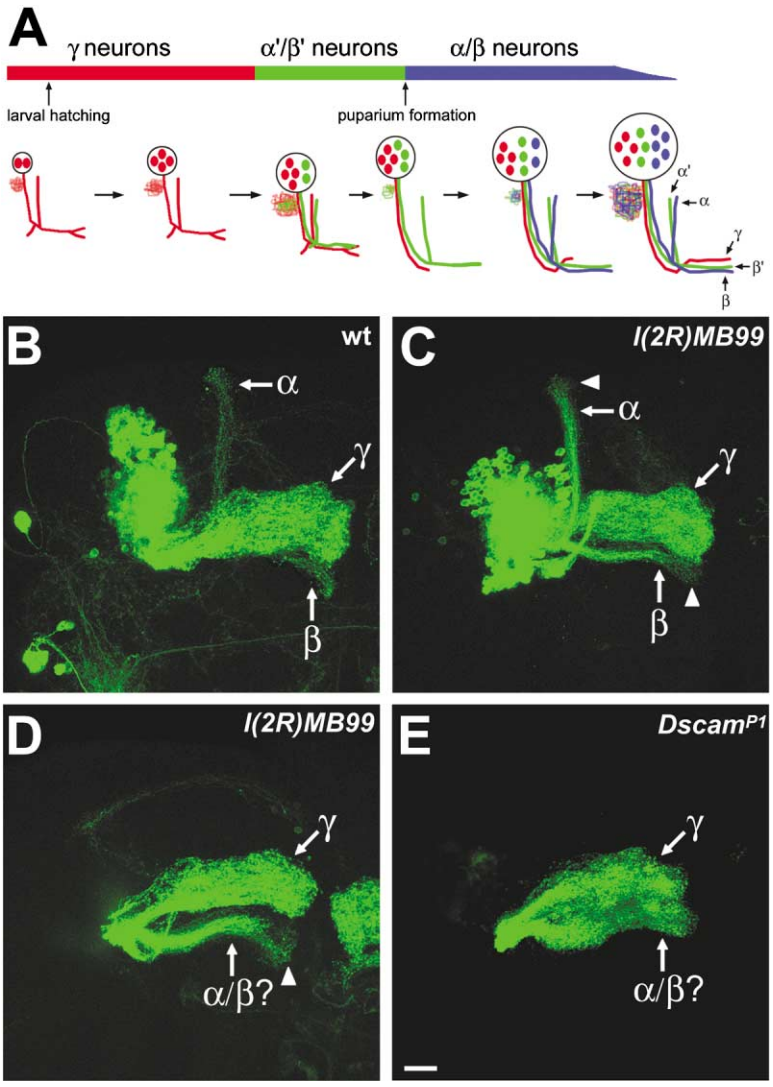

Figure 1. A Novel *Dscam* Mutation, *l(2R)MB99* (*Dscam*^{18}), as Well as a P Element-Mediated *Dscam* Mutation (*Dscam*^{P1}) Selectively Affect Formation of Bifurcated Axons in MB Clones

(A) shows a summary of the mushroom body development (adapted from Lee et al., 1999). Three distinct types of neurons, γ neurons (red), α'/β' neurons (green), and α/β neurons (blue) are sequentially derived from common precursors. At the adult stage, γ axons project medially without dorsal branching, while the α'/β' and α/β axons form separate sets of dorsal and medial bundles.

(B–E) Shown are composite confocal images of Adult MB Nb clones that were generated in newly hatched larvae (NHL). γ neurons and a small subset of α/β neurons are selectively labeled due to GAL4-201Y-driven expression of mCD8-GFP. Therefore, in wild-type (B), we observe full γ and weak α and β lobes. Interestingly, in *Dscam* mutant clones (C to E), the core α/β lobes are much denser and often fail to project away from each other (D and E). Note most processes do not reach the ends of α/β lobes (arrowheads) in some mutant clones. Similar numbers of cell bodies (about 200) are labeled in both wild-type and mutant clones. For clarity, only the lobe regions are shown in (D) and (E).

Genotype: (B) *hs-FLP/X ; FRTG13,UAS-mCD8-GFP,GAL4-201Y/FRTG13,tubP-GAL80*; (C and D) *hs-FLP/X ; FRTG13,l(2R)MB99,UAS-mCD8-GFP,GAL4-201Y/FRTG13,tubP-GAL80*; (E) *hs-FLP/X; FRTG13,Dscam*^{P1}*,UAS-mCD8-GFP, GAL4-201Y/FRTG13,tubP-GAL80*.

The scale bar in this and all figures (unless otherwise indicated) equals 20 μm. All unilateral MB clones are oriented such that their processes extend from left to right toward the midline. All images are processed from composite confocal images.

dures). Then, complementation against several deficiency lines allowed us to assign it to the interval between 43A3 and 43C3. Saturated mutagenesis has been conducted and only eight complementation groups exist within the 43A3-43C3 region (Heitzler et al., 1993). By performing complementation tests with existing lethal lines, we found that the *l(2R)MB99* mutant failed to complement with both *Dscam*^{1} and *Dscam*^{P1} lethal lines. To confirm that all *l(2R)MB99* phenotypes resulted from the loss of the Dscam activity, we created MB clones homozygous for the P element-induced *Dscam* mutation (*Dscam*^{P1}) and observed similar abnormalities in the α/β axons (e.g., Figure 1E). Taken together, we present a novel *Dscam* mutation (*Dscam*^{18}) that causes various defects in the MB lobes that are composed of bifurcated axons, indicating the involvement of the *Drosophila* Down syndrome cell adhesion molecule in the formation and guidance of axonal branches.

Misguidance of Wild-Type Axons due to Non-Cell-Autonomous Effects of *Dscam*$^{-/-}$ Clones

When *Dscam* mutant Nb clones are generated in NHL, the core α/β lobes always project in certain distinct patterns, including two bundles extending perpendicularly or in parallel, or only one bundle extending either dorsally or medially (Figures 1C–1E, 2D, and 2G). Given that one MB is derived from four indistinguishable cell lineages (Ito et al., 1997), we wondered whether a specific projection pattern observed in a given mutant clone was acquired as a result of changes in the overall MB morphologies.

To compare the projections of MARCM-labeled α/β axons with the projections of other α/β axons in the same MB, we selectively stained the entire α/β lobes using the anti-FasII monoclonal Ab 1D4 (Crittenden et al., 1998). If *Dscam* mutant Nb clones are generated in NHL, consistent projections are always observed between the MARCM-labeled α/β axons and the 1D4-stained α/β lobes, regardless of their projection patterns (Figure 2). When the mutant core α/β lobes extend as two distinct bundles side by side, all of the wild-type α/β processes, labeled as strong 1D4-positive fascicles, also project in the same direction as the mutant ones (Figures 2D–2F; n = 10). In such mosaic MBs, the two distinct bundles of MARCM-labeled core α/β axons, in addition to being in parallel, appear to extend along the center of two separate 1D4-positive lobes. Therefore,

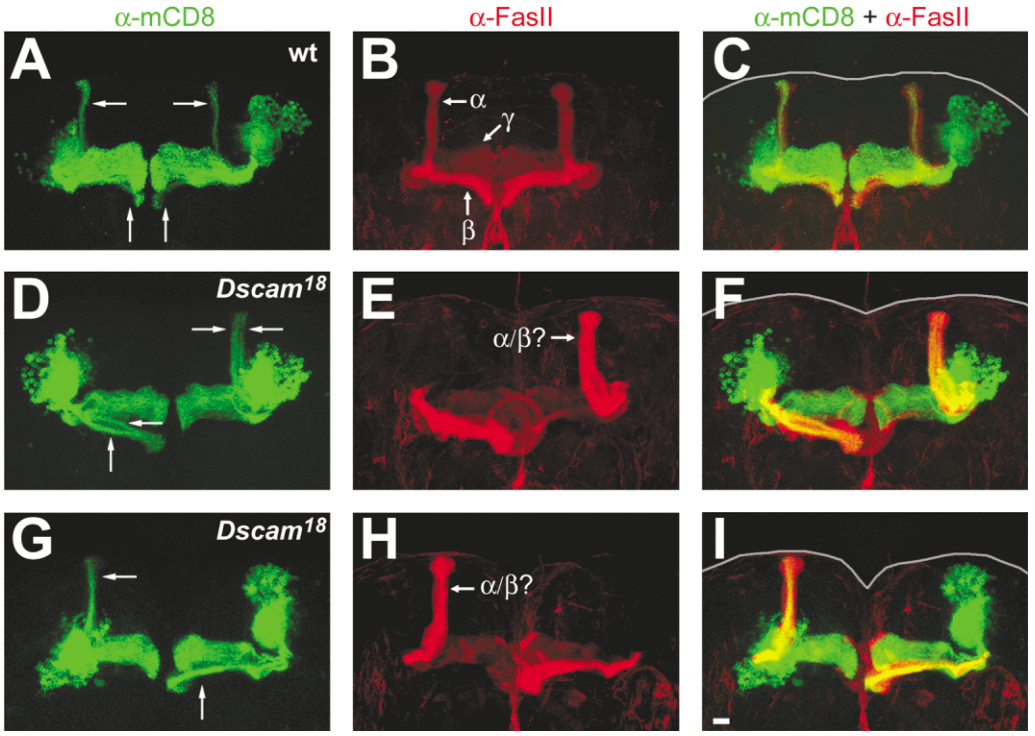

Figure 2. One *Dscam*[18] Homozygous Clone Can Affect the Projections of the Wild-Type Clones in the Same MB

Shown are adult brains containing pairs of MB Nb clones that were generated in NHL and examined in adults. MARCM clones were marked as GFP-positive cells (green), while the entire γ and α/β lobes were stained using the 1D4 mAb (red). (C), (F), and (I) are merged from (A) and (B), (D) and (E), and (G) and (H), respectively. In wild-type clones (A), the core α/β axons bifurcate into two bundles (arrows), one projects dorsally and the other projects toward the midline. In contrast, the core α/β neurons in *Dscam* mutant clones (D and G) fail to project axons in divergent directions. They can be fasciculated into two bundles (arrows) extending in parallel either dorsally or medially (D); or exist in a single bundle (arrows) that projects either dorsally or medially (G). Interestingly, the abnormal projections are followed by the wild-type α/β axons in mosaic MBs, as indicated by consistent changes in the α/β lobe morphology (strong red in [E] and [H]). Brains are outlined by gray curves.

Genotype: (A–C) *hs-FLP/X; FRTG13,UAS-mCD8-GFP,GAL4-201Y/FRTG13,tubP-GAL80*; (D–I) *hs-FLP/X; FRTG13,l(2R)MB99,UAS-mCD8-GFP,GAL4-201Y/FRTG13,tubP-GAL80*.

failure to achieve perpendicular segregation between the α and β lobes is seen in both mutant and wild-type clonal units within the same MBs. Moreover, when only one fascicle of mutant core α/β processes is observed in a given MB, the entire 1D4 bundle surrounding the mutant core α/β looks like only one lobe, indicating that an entire lobe is missing in such mosaic MBs (Figures 2G–2I; n = 9). The gross changes in the entire MB α/β lobes are always associated with *Dscam* mutant Nb clones, arguing against the notion that these global MB anomalies resulted from partial loss of Dscam activity in the heterozygous organisms. Taken together, these non-cell-autonomous effects suggest that *Dscam* mutant axons can somehow dictate the projections of wild-type axons in mosaic MBs. Moreover, consistent projection changes must be maintained in all follower processes, including both wild-type and mutant axons, within such mosaic MBs. In the following experiments, we tried to determine the mechanisms underlying these non-cell-autonomous effects, to identify primary cell-autonomous defects in *Dscam* mutant neurons, and to study the various phenotypes with single-axon resolution.

Consistent Guidance Defects Observed in Both α/β and α'/β' Lobes

Like α/β axons, α'/β' axons bifurcate into two lobes, one projecting dorsally and the other projecting medially toward the midline (Crittenden et al., 1998; Lee et al., 1999). Since the loss of Dscam activity affects divergent guidance of the bifurcated α/β axons, we wondered whether *Dscam*$^{-/-}$ α'/β' axons had the same problem. In order to visualize the α/β and α'/β' lobes simultaneously, we labeled MARCM clones using GAL4-OK107, which drives GAL4 expression in all MB neurons (Connolly et al., 1996). When clones are induced in NHL and examined in adults, consistent projection patterns are observed in all bifurcated axons, including α/β as well as α'/β' axons (Figures 3C and 3D, compared with Figures 3A and 3B). When all α/β axons project uni-directionally, either medially or dorsally, the α'/β' axons always extend uni-directionally and in the same direction as the α/β axons (n = 14). This phenomenon indicates that Dscam is required for axon bifurcation and guidance in both α/β and α'/β' neurons. Since α'/β' neurons are generated before α/β neurons (Lee et al., 1999) and they always acquire similar projection patterns, it is likely that the α'/β' axons play a key role in determining the

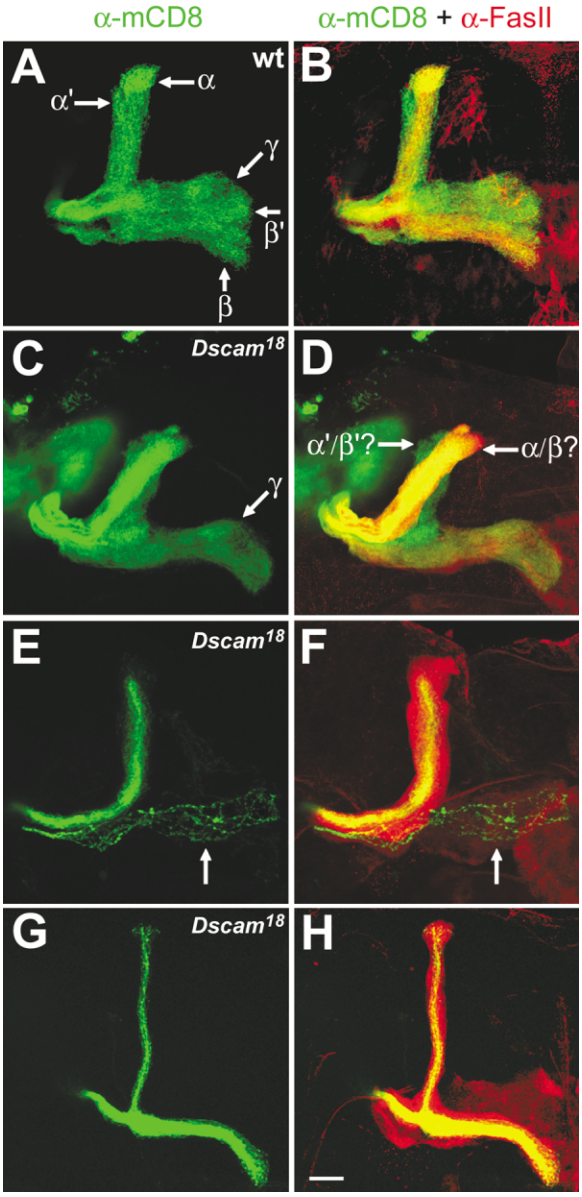

Figure 3. Phenotypic analysis of *Dscam* Mutant Mushroom Body Neuroblast Clones

(A–D) Consistent abnormalities are observed in the projections of α'/β' and α/β axons. Adult MB clones (green) were labeled using GAL4-OK107 in the MARCM system. The MB lobes as well as part of peduncle are selectively shown. Lobe identities were revealed by immunostaining with the 1D4 mAb (red in [B] and [D]). Clones were induced in NHL and examined in adults. In the wild-type clone (A and B), two lobes, α (green + strong red) and α' (green only), project dorsally and three lobes, β (green + strong red), β' (green only), and γ (green + weak red), project medially toward the midline. In contrast, only one lobe (γ) extends medially while the others extend dorsally in the *Dscam* mutant clone (C and D).

(E–H) Clone induction before and after initiation of α'/β' neuron production causes different patterns of abnormal projections. MB lobes in GAL4-201Y-labeled MARCM clones (green) are shown. The entire γ and α/β lobes were stained using 1D4 mAb (red in [F] and [H]). Clones were induced around the mid-3rd instar stage and examined in adults. Changes in the α/β lobe configuration (E and F) are found when mutant clones contain γ axons (arrows in [E] and [F]). In contrast, if mutant clones are induced after initiation of α'/β' neuron production (G and H), normal organization of α/β lobes is observed despite uneven segregation of axonal branches.

Genotype: (A and B) *hs-FLP/X; FRTG13,UAS-mCD8-GFP/FRTG13,tubP-GAL80; GAL4-OK107/+*; (C and D) *hs-FLP/X; FRTG13,I(2R)MB99,UAS-mCD8-GFP/FRTG13,tubP-GAL80 ; GAL4-OK107/+*; (E–H) *hs-FLP/X; FRTG13,I(2R)MB99,UAS-mCD8-GFP, GAL4-201Y/FRTG13,tubP-GAL80*.

projection patterns of the α/β axons in both wild-type and mutant MBs (see Discussion).

Timing of Clone Induction Affects *Dscam*$^{-/-}$ Phenotypes

Given that α'/β' axons determine the projection patterns of α/β axons, we wondered what would happen to *Dscam*$^{-/-}$ α/β axons if mutant clones were induced after establishment of wild-type α'/β' projections. To address this question, we created Nb clones at different developmental stages by controlling the timing of mitotic recombination. The entire α/β lobes as well as the mutant core α/β axons were examined simultaneously. If clones were generated right before the production of α'/β' neurons and consequently contained very few γ processes, non-cell-autonomous defects in the MB lobe configuration were observed in about 32% of the mosaic MBs (Figures 3E and 3F; n = 22). Therefore, similar phenotypic patterns are observed in all mosaic MBs, as long as mitotic recombination is induced before the establishment of α'/β' projections. In contrast, when mutant clones were created after the birth of α'/β' neurons, no non-cell-autonomous effects on the organization of the α/β lobes could be detected (Figure 3H). When clones were induced at the late 3rd instar stage, the α lobe projected dorsally while the β lobe projected medially toward the midline in all examined mosaic MBs (n = 68). However, despite the presence of both α and β lobe targets, mutant core α/β processes were unevenly distributed between the α and β lobes in about 30% of clones (Figures 3G and 3H). Taken together, these results are consistent with the idea that the first several α'/β' neurons serve as pioneer neurons that determine the configuration of MB lobes, which then influence the projections of later-born neurons regardless of their genotypes. In addition, abnormal segregation persisted in the mutant core α/β axons despite lack of non-cell-autonomous defects (Figures 3G and 3H), confirming Dscam's cell-autonomous functions in the divergent guidance of bifurcated axons.

Single-Cell Clones of *Dscam*$^{-/-}$ Neurons Exhibit Supernumerary Branches that Are Randomly Segregated

To address further the cell-autonomous and stage-specific involvement of Dscam in the formation and guidance of axonal branches, we knocked out wild-type *Dscam* from isolated single neurons by creating *Dscam* mutant single-cell clones of MB neurons within otherwise phenotypically wild-type organisms. Single neuron analysis reveals individual axonal branches and their trajectories, which is essential for detailed morphological analysis of *Dscam* mutant neurons.

Isolated single-cell/two-cell clones of MB neurons were created and specifically labeled using MB GAL4s in the MARCM system after brief heat shock at selected

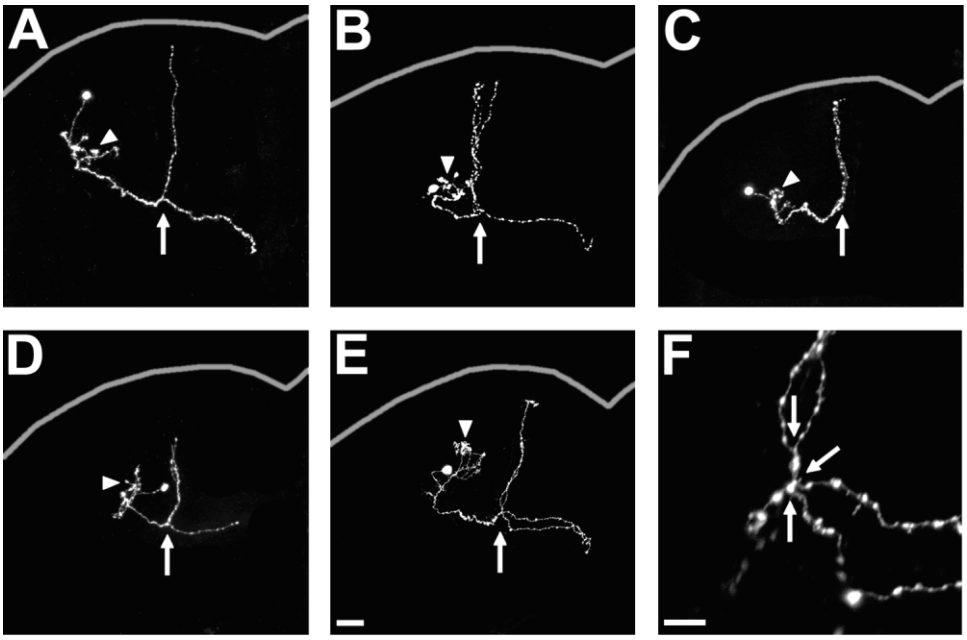

Figure 4. Single-Cell Clones of *Dscam* Mutant α/β Neurons Acquire Supernumerary Branches that Are Randomly Segregated

(A–E) Single-cell clones of wild-type (A) or *Dscam*$^{-/-}$ (B to E) α/β neurons were generated by inducing mitotic recombination after PF. As compared with the wild-type neuron (A) that projects one axon branch dorsally and the other medially toward the midline after forming two branches at the peduncle end (arrow), *Dscam* mutant neurons (B–E) often generate additional branches at the bifurcation points (arrows) and randomly project their axonal branches. Three dorsal branches/one medial branch, two dorsal branches only, two dorsal branches/one medial branch, and two dorsal branches/two medial branches are found in (B), (C), (D), and (E), respectively. In addition, axonal branches stop short in the *Dscam* mutant neuron (D) that was born within one day before eclosion. Note no detectable changes in the dendritic elaboration (arrowheads). Brains are outlined by gray curves.

(F) The region of axon bifurcation in (E) is shown as a single confocal image with higher magnification. Three bifurcation points (arrows) could be resolved spatially, and no more than two processes were derived at each branching point. The scale bar equals 5 μm.

Genotype: (A) *hs-FLP/X ; FRTG13,UAS-mCD8-GFP/FRTG13,tubP-GAL80 ; GAL4-OK107/+*; (B–F) *hs-FLP/X ; FRTG13,l(2R)MB99,UAS-mCD8-GFP/FRTG13,tubP-GAL80 ; GAL4-OK107/+*.

developmental stages. Clone induction in young larvae, wandering larvae, and pupae generated labeled γ, α'/β', and α/β neurons, respectively (Lee et al., 1999). When examined at the adult stage, *Dscam* mutant γ neurons look indistinguishable from wild-type γ neurons and project axons toward the midline without dorsal branching (data not shown). In contrast, *Dscam* mutant α'/β' and α/β neurons acquire obvious abnormalities in their axon branching and projecting patterns. Unlike wild-type axons that consistently bifurcate into two processes (Figure 4A; 100%, n = 50), mutant α'/β' and α/β axons often give rise to supernumerary branches (Figures 4B, 4D, and 4E; 42%, n = 80). These branches appear to be derived through repeated bifurcation at the peduncle end (Figure 4F; 100%, n = 10) and project toward the termini of MB lobes. In addition, these extra branches still acquire their cell type-specific morphological features, and mutant α/β axons are never incorporated into the α', β', or γ lobes, suggesting no cell fate change in *Dscam* mutant neurons. However, individual neurons sometimes fail to send processes into both dorsal and medial lobes (Figure 4C; 36%, n = 80). Such guidance defects seem to result from random distribution of mutant branches among the accessible lobes. In addition, extension of axonal branches is defective in most *Dscam* mutant α/β neurons that are generated within one day before eclosion (Figure 4D; 57%, n = 40). Taken together, these phenotypic studies of single-cell/two-cell clones not only confirm the cell-autonomous requirement of Dscam for proper segregation of sister branches, but also demonstrate the essential roles of Dscam in suppressing formation of additional branches.

Analysis of Mutant Nb Clones with Single-Cell Resolution Using "Flip-Out MARCM"

Because about 60% of *Dscam* mutant Nb clones look phenotypically wild-type while most single-cell clones of *Dscam* mutant α/β neurons have abnormal branching and projection patterns, we suspected that the individual axon trajectories were abnormal in these wild-type looking Nb clones. In order to examine individual axons in multicellular Nb clones, we marked only one or two neurons within each Nb clone using a flip-out GAL4 in the MARCM system (see Experimental Procedures; Figure 5A). We also labeled the MB lobes using the 1D4 mAb, which allowed us to examine the configuration of α/β lobes along with the single axons.

Irrespective of the lobe configuration, all of the mutant α/β axons, when examined as isolated single axons in Nb clones, yield multiple branches that extend randomly into the accessible lobes. Although the mutant α/β axons make two indistinguishable lobes in most of the Nb clones, their individual axons frequently send most or even all of their supernumerary branches into only one

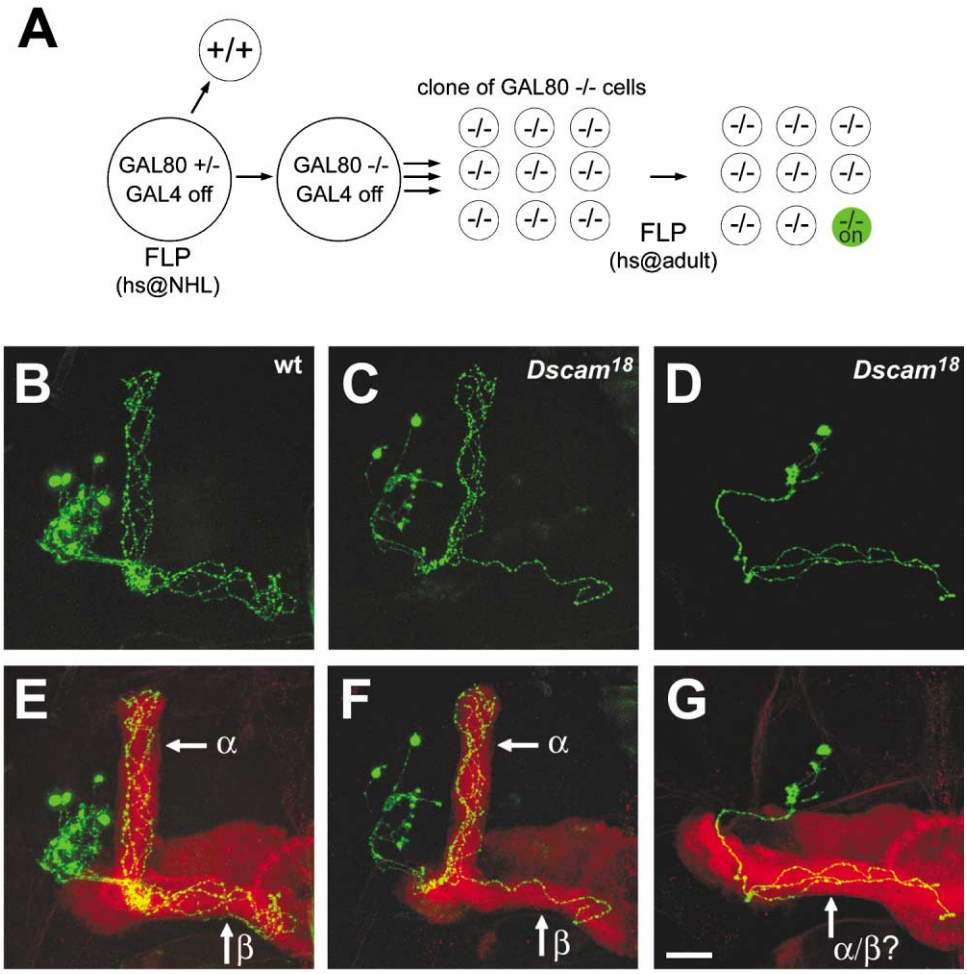

Figure 5. Single-Axon Analysis of Nb Clones Using "Flip-Out MARCM"

(A) shows a schematic illustration for selective labeling of single neurons within GAL80-minus Nb clones.

Heat shock-induced FLP activity mediates mitotic recombination in MB Nbs in newly hatched larvae (NHL). Through asymmetric division, GAL80-minus Nbs generate clones of GAL80-minus neurons. Then, a second heat shock is applied at the adult stage in order to turn on GAL4 expression in a small number of random cells, in which the FRT cassette is excised from the Flip-out GAL4 transgene. Because of suppression of GAL4 activity by GAL80, only GAL4-positive cells within clones of GAL80$^{-/-}$ neurons become specifically labeled.

(B–G) Single MB neurons (green) were specifically labeled within GAL80-minus Nb clones. The MB α/β lobes in (B) to (D) are revealed as strong mAb 1D4-stained bundles (bright red) in (E) to (G), respectively. Four α/β neurons are selectively marked in a wild-type clone (B and E), and four processes are observed in both α and β lobes. In contrast, two α/b neurons send five processes into the α lobe and only one process into the β lobe in a *Dscam* mutant Nb clone (C and F). In addition, when the α/β lobes are fused into one bundle (bright red in [G]), three branches are still derived from a single *Dscam* mutant α/β neuron (D and G).

Genotypes: (B and E) *Act>CD2>GAL4/hs-FLP; FRTG13,UAS-mCD8-GFP/FRTG13,tubP-GAL80*; the rest, *Act>CD2>GAL4/hs-FLP; FRTG13,l(2R)MB99,UAS-mCD8-GFP/FRTG13,tubP-GAL80*.

of the lobes (Figures 5C and 5F, compared with Figures 5B and 5E; n > 20). In addition, multifurcation of mutant axons at the original branching point persists even when the α/β fascicle is not bifurcated (Figures 5D and 5G; n = 8). Consistent with the morphological phenotypes of single-cell clones (Figure 4), these results indicate that loss of Dscam activity results in excessive axon branching and that *Dscam* mutant axons are defective in divergent guidance of axonal branches.

Single Axon Analysis of the Non-Cell-Autonomous Effects of *Dscam*$^{-/-}$ Clones

Because the organization of MB lobes has little bearing on the trajectories of individual axons (Figures 4 and 5), it is important to examine the non-cell-autonomous effects of *Dscam*$^{-/-}$ clones with single axon resolution as well. To analyze single wild-type axons in mosaic MBs, we created a mutant Nb clone within each MB at the early larval stage and then generated single-cell clones of wild-type α/β neurons in the same MB after PF (Figure 6A). Using "reverse MARCM," in which the mutation of interest and the *tubP-GAL80* transgene are on the same chromosome arm, we selectively labeled the daughter cell that is wild-type after the mitotic recombination event (Lee et al., 2000b). Thus, when mitotic recombination was induced in NHL, formation of mutant Nb clones led to specific labeling of two-cell clones of wild-type γ neurons. Then, induction of mitotic recombi-

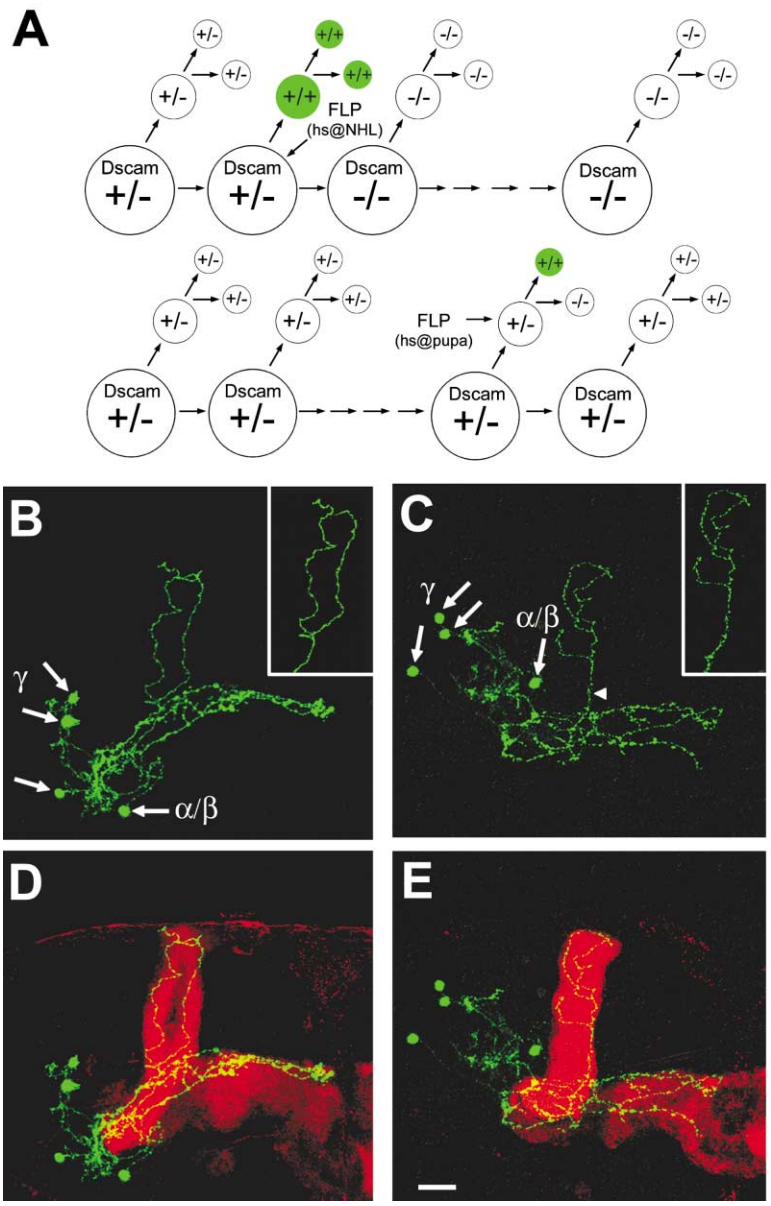

Figure 6. "Reverse MARCM" for Examining Dscam's Non-Cell-Autonomous Effects with Single Neuron Resolution

(A) Schematic illustration for labeling isolated wild-type neurons in mosaic MBs.

Two of the four cell lineages in one MB are selectively shown. When mitotic recombination in NHL lead to formation of one homozygous mutant Nb, a two-cell clone of γ neurons becomes specifically labeled because of loss of GAL80 from homozygous wild-type cells in the reverse MARCM system. Then, a second heat shock is conducted at the pupal stage in order to label single-cell clones of wild-type α/β neurons that are derived from other lineages within the same MB.

(B–E) GFP-positive wild-type MB neurons (green) were created according to the scheme described in (A). Three γ neurons, including one two-cell clone, as well as one α/β neuron are specifically labeled in each MB. Staining with the 1D4 mAb reveals the organization of the MB lobes (red in [D] and [E]). When the α/β lobes project as two parallel bundles (D), the wild-type α/β axon bifurcates and sends one process into each bundle (B and D). In contrast, when there is only one α/β bundle (E), the α/β axon projects into the α/β bundle as a single process (C and E; arrowhead in [C]) without bifurcation. For closer inspection, both α/β axons are separately shown (insets in [B] and [C]). Note presence of side branches in the nonbifurcated α/β axon.

Genotype: *hs-FLP/X ; FRTG13,UAS-mCD8-GFP/FRTG13,l(2R)MB99,tubP-GAL80; GAL4-OK107/+*.

nation again at the pupal stage yielded single-cell clones of wild-type α/β neurons that were specifically marked within the MBs already containing Nb clones of mutant neurons. We also labeled the whole MB lobes using the 1D4 mAb in order to compare single axon trajectories with the organization of α/β lobes.

We examined single wild-type α/β axons in the mosaic MBs containing mutant Nb clones. In contrast with *Dscam* mutant α/β axons that acquire diverse branching and projecting patterns (Figures 4B–4E), individual wild-type axons project in a predictable pattern that is consistent with the α/β lobe configuration. As expected, wild-type α/β axons undergo bifurcation and send one branch into each lobe when there are two distinct lobes (Figures 6B and 6D; $n > 10$). When only one lobe remains, we observe that the wild-type α/β axons extend without bifurcation (Figures 6C and 6E; $n > 10$). These results indicate that wild-type α/β axons undergo minimal branching and always project their branches divergently even after the gross organization of MB lobes is altered by *Dscam* mutant Nb clones.

Dscam Is Specifically Required for Axon Arborization in Two Distinct Types of Elliposid Body Neurons

To check whether Dscam is widely involved in formation and guidance of axonal branches, we then examined non-MB MARCM clones using one of our enhancer-trap GAL4 lines that labels a subset of ellipsoid body (EB) neurons. The EB is one of the four neuropils of the central complex, which lays at the junction of the two brain lobes. Using this EB GAL4 line in the MARCM system, we have identified two types of neurons that are distinguished based on their axon arborization patterns. Some axons establish circular trajectories and form repeated discrete arbors inward along the entire circle

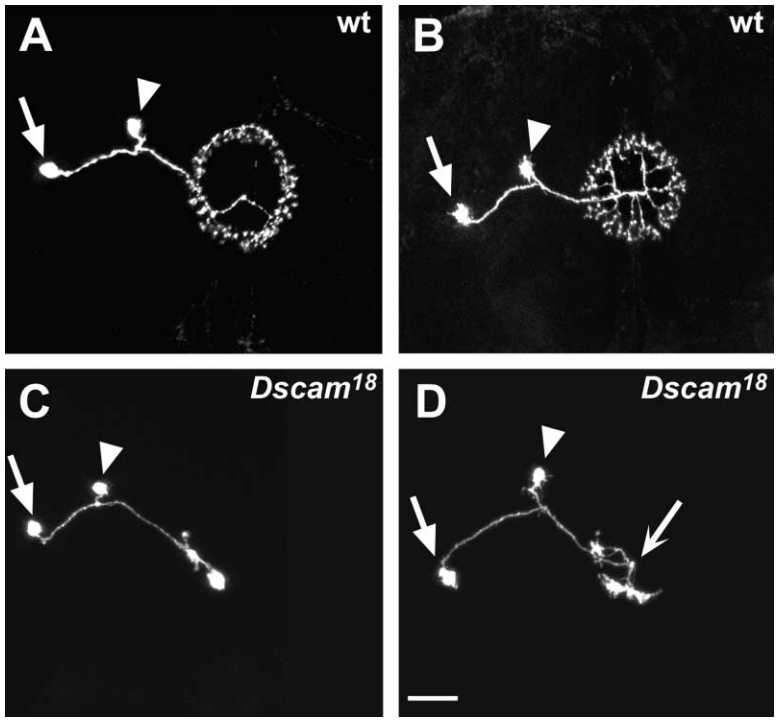

Figure 7. Dscam Activity Is Essential for Axon Arborization within the Ellipsoid Body (EB)

Single axon analysis using an EB-specific GAL4 in MARCM. Two types of EB neurons can be distinguished based on their distinct axon arborization patterns—one with a circular trajectory (A) and the other with an axial trajectory (B). In contrast, *Dscam* mutant axons appear to be arrested at the beginning of their arborization processes (C and D). Note no defect in their initial pathfinding; and the mutant axon in (D) but not the one in (C) arrives at the EB's center (concave arrow). Cell bodies and dendrites are indicated by arrows and arrowheads, respectively.

Genotype: (A and B) *hs-FLP/X ; FRTG13,UAS-mCD8-GFP/FRTG13,tubP-GAL80; GAL4-EB1/+*; (C and D) *hs-FLP/X ; FRTG13,Dscam^{18},UAS-mCD8-GFP/FRTG13,tubP-GAL80; GAL4-EB1/+*.

(Figure 7A), while others project to the EB center before branching into multiple processes that radiate outward and end with nonoverlapping arborization around the EB (Figure 7B). To determine the roles of Dscam in the formation of distinct axon arborization patterns, we selectively knocked out Dscam activity from these EB neurons by creating *Dscam* mutant single-cell clones. We observe that mutant neurons fail to elaborate their axon projections within the EB despite normal initial pathfinding (Figures 7C and 7D). It appears that *Dscam* mutant axons generate supernumerary branches that tangle together as they attempt to arborize. This is consistent with Dscam's essential role in mediating divergent segregation of sister branches and suppression of ectopic bifurcation in mushroom body neurons.

Discussion

Requirement of Dscam for the Bifurcation of MB Lobes

We demonstrate that Dscam is involved in regulating the bifurcation of MB axons. Instead of having two branches that project away from each other, *Dscam* mutant axons give rise to supernumerary branches, through repeated bifurcation, that fail to extend in divergent directions. Interestingly, the *Drosophila Dscam* gene potentially encodes tens of thousands of isoforms with distinct extracellular domains (Schmucker et al., 2000). It is likely that homophilic interactions between identical Dscam molecules (Agarwala et al., 2000) mediate novel mechanisms that coordinate induction of axon bifurcation with segregation of sister branches. In addition, we observe that *Dscam* mutant axons can alter the projections of wild-type axons within the same MB. Further investigations into the cellular basis of such non-cell-autonomous effects will shed new light on how the insect olfactory learning and memory center acquires its normal projection patterns during development.

A Model for Dscam-Regulated Formation and Segregation of Axonal Branches

Several different scenarios can account for the observed correlation of ectopic bifurcation with abnormal segregation in *Dscam* mutant axons. One possibility is that Dscam activity might play a direct role in both divergent segregation of sister branches and suppression of ectopic bifurcation. These two activities could occur via a common mechanism or through two independent signaling events. Alternatively, the role of Dscam in divergent segregation of sister branches could be a secondary consequence of its suppression of axon bifurcation, or vice versa. We favor the idea that Dscam directly controls both formation and segregation of axonal branches because in single mutant cells, abnormal segregation is not always coupled with the generation of additional branches and vice versa. Most likely, Dscam normally prevents sister branches from extending along the same path and consequently suppresses additional bifurcation after the sister branches have occupied all available paths.

One mechanism that can explain coordination of axon bifurcation with divergent segregation is Dscam-dependent growth cone collapse. When sister growth cones contact each other, homophilic interactions between Dscam molecules (Agarwala et al., 2000) may lead to growth cone collapse or fusion (Figure 8). Thus, when axons bifurcate, only divergently split growth cones could survive, initiating separation of sister branches. Moreover, new growth cones continue to bifurcate until all target sites receive branches; but only one growth cone derived from any individual neuron could traverse a given path because the Dscam-mediated homophilic

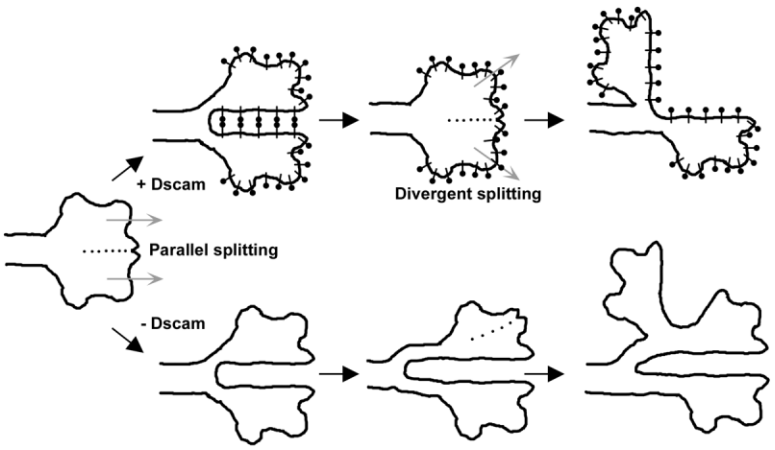

Figure 8. A Model for Dscam-Regulated Axon Bifurcation

When a growth cone is induced to divide, it can undergo parallel splitting or divergent splitting. (Top) However, if the split growth cones are extending along the same path, they will be collapsed back to one due to homophilic interactions between the Dscam molecules. As a result, only twin growth cones projecting in divergent directions can survive and lead to the formation and segregation of sister processes. Such Dscam-mediated collapse of growth cones also inhibits additional bifurcation after all accessible paths have been taken. (Bottom) In contrast, twin growth cones can extend along the same path independently in the absence of Dscam molecules. Moreover, *Dscam* mutant axons often acquire supernumerary branches via repeated bifurcation.

interactions would immediately collapse adjacent sister growth cones into one. This mechanism would couple formation of axonal branches to divergent guidance of sister branches. The final result would be that individual axons would innervate multiple targets through minimal bifurcation. In contrast, sister branches may extend along the same path after loss of Dscam activity. Consequently, when bifurcation is induced in mutant axons, they randomly distribute their branches and often generate additional branches through repeated bifurcation.

This model also suggests that induction of axon bifurcation may not always lead to formation of sister branches. Growth cones split in response to bifurcation-inducing signals. However, if twin growth cones cannot migrate divergently, then no axon bifurcation would be expected after futile cycles of splitting followed by collapse. This mechanism can explain why bifurcation is suppressed in wild-type axons when only one trajectory is left (Figures 6C and 6E). Despite the lack of bifurcated bundles, induction of axon bifurcation persists in mosaic MBs since *Dscam* mutant axons still generate multiple branches at the original bifurcation point (Figures 5D and 5G). Taken together, these observations further support the proposal that divergent guidance is essential for the survival of twin growth cones in the presence of normal Dscam activity. To test this model directly, we are in the process of examining growth cone splitting in real time.

Possible Functions of Different Dscam Isoforms

Remarkably, *Drosophila* Dscam may exist in numerous isoforms through alternative splicing (Schmucker et al., 2000); and Dscam is widely required for axon arborization in distinct CNS neurons. Given that various Dscam isoforms exhibit distinct features in their extracellular domains while sharing common intracellular structures (Schmucker et al., 2000), it is likely that activation of a common Dscam-dependent signaling pathway is dynamically and differentially regulated in distinct growth cones expressing distinct sets of Dscam's. Although immunohistochemistry using an anti-Dscam Ab (Schmucker et al., 2000) revealed general expression of *Dscam* in most pupal brain structures (data not shown), it remains unclear whether distinct Dscam isoforms are expressed in different neurons. However, delicate cell type-specific controls of Dscam signaling could be achieved if homophilic interactions were restricted to identical or certain pairs of Dscam isoforms. In addition, activation of Dscam might lead to different developmental changes, depending on the types of cellular structures that are involved. For instance, Dscam-Dscam interactions between split growth cones may result in reunification of growth cones. In contrast, homophilic Dscam binding could mediate contact-dependent attraction of growth cones when the interactions occur between growth cones and their guiding substrates. Such Dscam-mediated growth cone guidance might be crucial to normal extension of GAL4-201Y-positive α/β neurons (Figure 4D) as well as correct pathfinding of the Bolwig's nerve (Schmucker et al., 2000). If the Dscam pathway is widely used to mediate various growth cone behaviors, it is understandable that numerous Dscam isoforms would be needed to confer diverse activation patterns in different types of growth cones.

Roles of Pioneer Axons in the Configuration of MB Lobes

Analysis of the non-cell-autonomous effects of *Dscam* mutant clones convinces us that the first-born α'/β' neurons play a crucial role in shaping the projection patterns of all later-born MB neurons. If Nb clones are induced after the initiation of α'/β' neuron production, we always observe both dorsal and medial MB lobes (Figure 3H). In contrast, if early α'/β' neurons are made homozygous for a *Dscam* mutation, absence of either the dorsal or medial lobe is observed in about one-third of mosaic MBs (Figures 2E, 2H, and 3F). Interestingly, consistent patterns exist between α'/β' lobes and α/β lobes (Figure 3C). Given that α'/β' neurons, unlike γ neurons, maintain their projection patterns through metamorphosis (Lee et al., 1999), the effects of early α'/β' neurons on the final organization of MB lobes support roles of α'/β' axons as pioneer axons that guide the projections of adult-specific MB neurons. Because α'/β' axons and α/β axons form distinct bundles (Crittenden et al., 1998; Lee et al., 1999), the effects of α'/β' axons on the projections of α/β axons may be due to pioneer axon-mediated changes in the arrangement of local glial cells (Jhaveri et al., 2000). Since one MB is composed of four indistin-

guishable clonal units (Ito et al., 1997), how several cells within one unit can dominate the entire MB projection patterns remains to be elucidated.

Our demonstration of *Drosophila* Dscam's essential roles in the bifurcation of MB axons immediately suggests many lines of research for future investigation of the molecular mechanisms underlying growth cone splitting. For instance, it remains to be determined whether the Dock/Pak signaling pathway is involved in bifurcation of various axons. In addition, it is uncertain whether the vertebrate Dscam (Yamakawa et al., 1998; Agarwala et al., 2001) plays similar roles during development of the CNS. Identification of additional molecules that control bifurcation of axons in *Drosophila* may generate new insights into how similar neuronal morphogenetic processes are regulated in vertebrates.

Experimental Procedures

Fly Strains

GAL80 fly stocks used for creation of MARCM clones include (1) *hs-FLP; FRTG13,tubP-GAL80/CyO* and (2) *UAS-mCD8-GFP,hs-FLP; FRTG13,tubP-GAL80/CyO; GAL4-OK107*. (3) *FRTG13,UAS-mCD8-GFP,GAL4-201Y*, (4) *Act>CD2>GAL4; FRTG13,UAS-mCD8-GFP,* and (5) *FRTG13,UAS-mCD8-GFP* were used for generating wild-type clones; while (6) *FRTG13,l(2R)MB99,UAS-mCD8-GFP, GAL4-201Y/CyO*, (7) *Act>CD2>GAL4; FRTG13,l(2R)MB99,UAS-mCD8-GFP/CyO*, (8) *FRTG13,l(2R)MB99,UAS-mCD8-GFP*, and (9) *FRTG13,Dscam^{P1}/CyO* were used for generating *Dscam* mutant clones. In addition, (10) *hs-FLP; FRTG13,l(2R)MB99,tubP-GAL80/CyO* and (11) *FRTG13,UAS-mCD8-GFP; GAL4-OK107* were used for "reverse MARCM." Generation of EB MARCM clones involves (12) *FRTG13,UAS-mCD8-GFP; GAL4-EB1* and (13) *FRTG13,Dscam^{18}*, UAS-mCD8-GFP; GAL4-EB1.

Other fly stocks collected for this study include *al,dp,b, pr,cn,c,px,sp/CyO* (a gift from J. McDonald), *Df(2R)pk78k/CyO* (BL-1594), *Df(2R)P32a/CyO* (BL-2467), *l(2)43Ba/CyO* (BL-4119), *pwn/Sm5* (BL-750), *l(2)43Bb/CyO* (BL-4118), *P{ry+}l(2)43Bb/CyO* (BL-11382), *Dscam^{P1}/CyO* (BL-11412), *cos/CyO* (BL-3919), *P{w+}cos/CyO* (BL-11156), *l(2)43Bd/CyO* (BL-4122), *hum/CyO* (BL-3921), *so/CyO* (BL-4287), and *l(2)43Bc/CyO* (gifts from J. Roote, University of Cambridge).

MARCM-Based Genetic Screens

Chemical mutagenesis was conducted in the *FRTG13,UAS-mCD8-GFP,GAL4-201Y* male flies using standard procedures (Lewis and Bacher, 1968) with an EMS concentration of 40 mM. Individual male progeny derived from the mutagenized flies were then crossed with *hs-FLP ; FRTG13,tubP-GAL80* for MARCM analysis of MB clones that were homozygous for the mutations induced on the *FRTG13,UAS-mCD8,GAL4-201Y* chromosome arms. These genetic crosses are summarized in the following scheme.

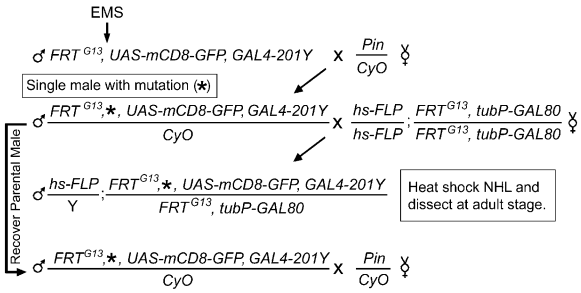

Mapping by Recombination and Complementation

After we knew that the *l(2R)MB99* line was homozygous lethal, we tried to determine whether the MB phenotypes in the *l(2R)MB99* mutant clones simply resulted from a lethal mutation. First of all, homologous recombination was induced between the *FRTG13,UAS-mCD8-GFP,GAL4-201Y* mutant chromosome and a second chromosome carrying multiple known mutations. Two regions of lethal mutation were easily separated—one lethal region was mapped around the 43 cytogenetic locus and the other on the 2L chromosome arm. MARCM analysis of various recombinant lines revealed that MB phenotypes were always associated with the lethal mutation(s) in the 43 region. Because the *l(2R)MB99* line failed to complement with two deficiency lines lacking the 43A3-C3 region in common, we then directly tested whether the *l(2R)MB99* mutation belonged to any of the eight complement groups within the region between 43A3 and 43C3 (Heitzler et al., 1993). Complementation assays finally assigned the *l(2R)MB99* mutation to the 43Bc group, indicating that *l(2R)MB99* is a new *Dscam* allele (*Dscam^{18}*).

Induction and Phenotypic Analysis of MARCM Clones

As a result of FLP-mediated site-specific mitotic recombination, MARCM clones of GAL80-minus cells were created from heterozygous precursors. Using the *hs-FLP* transgene, we induced mitotic recombination at selected stages by heat shock at 37°C. After clone induction at specific developmental stages, adult flies were dissected in cold phosphate-buffered saline and their brains were fixed and immunostained, as previously described (Lee et al., 1999, 2000b).

MARCM clones were detected by the rat anti-mCD8 mAb (1:100, Caltag) and MB lobes were labeled by the 1D4 mAb (1:80). Immunofluorescent signals were collected by confocal microscopy and then processed using Adobe Photoshop.

Single Axon Analysis in MARCM Nb Clones Using "Flip-Out MARCM"

Specific labeling of MARCM clones is basically achieved by GAL4-dependent expression of a marker gene in cells lacking GAL80 (Lee and Luo, 1999). In our other experiments, various tissue-specific enhancers control expression of GAL4. Thus, all GAL80-minus cells within GAL4-positive tissues were labeled. In order to mark a small subset of cells within the large MARCM clones, we took advantage of a flip-out GAL4 transgene (*Act > CD2 > GAL4*) (Lawrence et al., 1999). GAL4 expression from the flip-out construct is silent until excision of an FRT cassette unites a ubiquitous promoter with the GAL4 open reading frame. The FLP/FRT system is used for mediating both the mitotic recombination (Golic and Lindquist, 1989) and the flipping out (Struhl and Basler, 1993), but we found that these two events rarely occur simultaneously in proliferating cells and that only flipping out could occur in postmitotic cells. Therefore, we can selectively create GAL80-minus MB Nbs by heat shock induction of Flipase (FLP) activity in NHL. Then, some of the neurons in the GAL80-minus Nb clones undergo flipping out during a second heat shock at the adult stage (Figure 5A). The frequency of flipping out is dependent on the FLP activity.

Acknowledgments

We thank J. Roote for some of the known *Dscam* mutant flies; the Bloomington Stock Center for other mutant flies; C. Goodman for the 1D4 mAb; L. Zipursky for the anti-Dscam Ab; and M. Kim for assistance on confocal microscopy. We thank D. Montell, W.T. Greenough, A. Chiba, and members of the Lee lab for comments on the manuscript. C.T.Z. was supported as a trainee by an NIH grant (T32 GM07283). This work was supported by a start-up fund from the University of Illinois and a grant to T.L. from the National Institutes of Health (R01-NS42049).

Received August 16, 2001; revised November 29, 2001.

References

Acebes, A., and Ferrus, A. (2000). Cellular and molecular features of axon collaterals and dendrites. Trends Neurosci. *23*, 557–565.

Agarwala, K.L., Nakamura, S., Tsutsumi, Y., and Yamakawa, K. (2000). Down syndrome cell adhesion molecule DSCAM mediates homophilic intercellular adhesion. Brain Res. Mol. Brain Res. *79*, 118–126.

Agarwala, K.L., Ganesh, S., Amano, K., Suzuki, T., and Yamakawa, K. (2001). DSCAM, a highly conserved gene in mammals, expressed in differentiating mouse brain. Biochem. Biophys. Res. Commun. *281*, 697–705.

Bastmeyer, M., and O'Leary, D.D. (1996). Dynamics of target recognition by interstitial axon branching along developing cortical axons. J. Neurosci. *16*, 1450–1459.

Chen, H., He, Z., Bagri, A., and Tessier-Lavigne, M. (1998). Semaphorin-neuropilin interactions underlying sympathetic axon responses to class III semaphorins. Neuron *21*, 1283–1290.

Connolly, J.B., Roberts, I.J., Armstrong, J.D., Kaiser, K., Forte, M., Tully, T., and O'Kane, C.J. (1996). Associative learning disrupted by impaired Gs signaling in *Drosophila* mushroom bodies. Science *274*, 2104–2107.

Crittenden, J.R., Skoulakis, E.M., Han, K.A., Kalderon, D., and Davis, R.L. (1998). Tripartite mushroom body architecture revealed by antigenic markers. Learn. Mem. *5*, 38–51.

de Belle, J.S., and Heisenberg, M. (1994). Associative odor learning in *Drosophila* abolished by chemical ablation of mushroom bodies. Science *263*, 692–695.

Fashena, D., and Westerfield, M. (1999). Secondary motoneuron axons localize DM-GRASP on their fasciculated segments. J. Comp. Neurol. *406*, 415–424.

Gallo, G., and Letourneau, P.C. (1998). Localized sources of neurotrophins initiate axon collateral sprouting. J. Neurosci. *18*, 5403–5414.

Golic, K.G., and Lindquist, S. (1989). The FLP recombinase of yeast catalyzes site-specific recombination in the *Drosophila* genome. Cell *59*, 499–509.

Grotewiel, M.S., Beck, C.D., Wu, K.H., Zhu, X.R., and Davis, R.L. (1998). Integrin-mediated short-term memory in *Drosophila*. Nature *391*, 455–460.

Heisenberg, M., Borst, A., Wagner, S., and Byers, D. (1985). *Drosophila* mushroom body mutants are deficient in olfactory learning. J. Neurogenet. *2*, 1–30.

Heitzler, P., Coulson, D., Saenz-Robles, M.T., Ashburner, M., Roote, J., Simpson, P., and Gubb, D. (1993). Genetic and cytogenetic analysis of the 43A-E region containing the segment polarity gene *costa* and the cellular polarity genes *prickle* and *spiny-legs* in *Drosophila melanogaster*. Genetics *135*, 105–115.

Hidalgo, A., and Brand, A.H. (1997). Targeted neuronal ablation: the role of pioneer neurons in guidance and fasciculation in the CNS of *Drosophila*. Development *124*, 3253–3262.

Hong, K., Hinck, L., Nishiyama, M., Poo, M.M., Tessier-Lavigne, M., and Stein, E. (1999). A ligand-gated association between cytoplasmic domains of UNC5 and DCC family receptors converts netrin-induced growth cone attraction to repulsion. Cell *97*, 927–941.

Ito, K., Awano, W., Suzuki, K., Hiromi, Y., and Yamamoto, D. (1997). The *Drosophila* mushroom body is a quadruple structure of clonal units each of which contains a virtually identical set of neurones and glial cells. Development *124*, 761–771.

Ito, K., and Hotta, Y. (1992). Proliferation pattern of postembryonic neuroblasts in the brain of *Drosophila melanogaster*. Dev. Biol. *149*, 134–148.

Jhaveri, D., Sen, A., and Rodrigues, V. (2000). Mechanisms underlying olfactory neuronal connectivity in *Drosophila*-the atonal lineage organizes the periphery while sensory neurons and glia pattern the olfactory lobe. Dev. Biol. *226*, 73–87.

Kidd, T., Brose, K., Mitchell, K.J., Fetter, R.D., Tessier-Lavigne, M., Goodman, C.S., and Tear, G. (1998). Roundabout controls axon crossing of the CNS midline and defines a novel subfamily of evolutionarily conserved guidance receptors. Cell *92*, 205–215.

Kidd, T., Bland, K.S., and Goodman, C.S. (1999). Slit is the midline repellent for the robo receptor in *Drosophila*. Cell *96*, 785–794.

Lawrence, P.A., Casal, J., and Struhl, G. (1999). hedgehog and engrailed: pattern formation and polarity in the *Drosophila* abdomen. Development *126*, 2431–2439.

Lee, T., and Luo, L. (1999). Mosaic analysis with a repressible cell marker for studies of gene function in neuronal morphogenesis. Neuron *22*, 451–461.

Lee, T., and Luo, L. (2001). Mosaic analysis with a repressible cell marker (MARCM) for *Drosophila* neural development. Trends Neurosci. *24*, 251–254.

Lee, T., Lee, A., and Luo, L. (1999). Development of the *Drosophila* mushroom bodies: sequential generation of three distinct types of neurons from a neuroblast. Development *126*, 4065–4076.

Lee, T., Marticke, S., Sung, C., Robinow, S., and Luo, L. (2000a). Cell autonomous requirement of the USP/EcR-B ecdysone receptor for mushroom body neuronal remodeling. Neuron *28*, 807–818.

Lee, T., Winter, C., Marticke, S.S., Lee, A., and Luo, L. (2000b). Essential roles of *Drosophila* RhoA in the regulation of neuroblast proliferation and dendritic but not axonal morphogenesis. Neuron *25*, 307–316.

Lewis, E.B., and Bacher, F. (1968). Method of feeding ethylmethane sulfonate (EMS) to *Drosophila* males. Drosoph. Inf. Serv. *43*, 193.

Mason, C.A., and Wang, L.C. (1997). Growth cone form is behavior-specific and, consequently, position-specific along the retinal axon pathway. J. Neurosci. *17*, 1086–1100.

Matheson, S.F., and Levine, R.B. (1999). Steroid hormone enhancement of neurite outgrowth in identified insect motor neurons involves specific effects on growth cone form and function. J. Neurobiol. *38*, 27–45.

Moran-Rivard, L., Kagawa, T., Saueressig, H., Gross, M.K., Burrill, J., and Goulding, M. (2001). Evx1 is a postmitotic determinant of v0 interneuron identity in the spinal cord. Neuron *29*, 385–399.

Pierani, A., Moran-Rivard, L., Sunshine, M.J., Littman, D.R., Goulding, M., and Jessell, T.M. (2001). Control of interneuron fate in the developing spinal cord by the progenitor homeodomain protein Dbx1. Neuron *29*, 367–384.

Pike, S.H., Melancon, E.F., and Eisen, J.S. (1992). Pathfinding by zebrafish motoneurons in the absence of normal pioneer axons. Development *114*, 825–831.

Sato, M., Lopez-Mascaraque, L., Heffner, C.D., and O'Leary, D.D. (1994). Action of a diffusible target-derived chemoattractant on cortical axon branch induction and directed growth. Neuron *13*, 791–803.

Schmucker, D., Clemens, J.C., Shu, H., Worby, C.A., Xiao, J., Muda, M., Dixon, J.E., and Zipursky, S.L. (2000). *Drosophila* Dscam is an axon guidance receptor exhibiting extraordinary molecular diversity. Cell *101*, 671–684.

Scott, E.K., Lee, T., and Luo, L. (2001). enok encodes a *Drosophila* putative histone acetyltransferase required for mushroom body neuroblast proliferation. Curr. Biol. *11*, 99–104.

Shaw, G., Bray, D., Hidalgo, A., and Brand, A.H. (1977). Movement and extension of isolated growth cones. Exp. Cell Res. *104*, 55–62.

Song, H.J., and Poo, M.M. (1999). Signal transduction underlying growth cone guidance by diffusible factors. Curr. Opin. Neurobiol. *9*, 355–363.

Song, H., Ming, G., He, Z., Lehmann, M., McKerracher, L., Tessier-Lavigne, M., and Poo, M. (1998). Conversion of neuronal growth cone responses from repulsion to attraction by cyclic nucleotides. Science *281*, 1515–1518.

Strausfeld, N.J. (1976). Atlas of an Insect Brain (Berlin: Springer-Verlag).

Struhl, G., and Basler, K. (1993). Organizing activity of wingless protein in *Drosophila*. Cell *72*, 527–540.

Sugihara, I., Wu, H., and Shinoda, Y. (1999). Morphology of single olivocerebellar axons labeled with biotinylated dextran amine in the rat. J. Comp. Neurol. *414*, 131–148.

Tear, G., Harris, R., Sutaria, S., Kilomanski, K., Goodman, C.S., and Seeger, M.A. (1996). commissureless controls growth cone guidance across the CNS midline in *Drosophila* and encodes a novel membrane protein. Neuron *16*, 501–514.

Tessier-Lavigne, M., and Goodman, C.S. (1996). The molecular biology of axon guidance. Science *274*, 1123–1133.

Thor, S., Andersson, S.G., Tomlinson, A., and Thomas, J.B. (1999).

A LIM-homeodomain combinatorial code for motor-neuron pathway selection. Nature *397*, 76–80.

Truman, J.W., and Bate, M. (1988). Spatial and temporal patterns of neurogenesis in the central nervous system of *Drosophila melanogaster*. Dev. Biol. *125*, 145–157.

Wang, F., Nemes, A., Mendelsohn, M., and Axel, R. (1998). Odorant receptors govern the formation of a precise topographic map. Cell *93*, 47–60.

Wang, K.H., Brose, K., Arnott, D., Kidd, T., Goodman, C.S., Henzel, W., and Tessier-Lavigne, M. (1999). Biochemical purification of a mammalian slit protein as a positive regulator of sensory axon elongation and branching. Cell *96*, 771–784.

Winberg, M.L., Mitchell, K.J., and Goodman, C.S. (1998). Genetic analysis of the mechanisms controlling target selection: complementary and combinatorial functions of netrins, semaphorins, and IgCAMs. Cell *93*, 581–591.

Yamakawa, K., Huot, Y.K., Haendelt, M.A., Hubert, R., Chen, X.N., Lyons, G.E., and Korenberg, J.R. (1998). DSCAM: a novel member of the immunoglobulin superfamily maps in a Down syndrome region and is involved in the development of the nervous system. Hum. Mol. Genet. *7*, 227–237.

Yang, M.Y., Armstrong, J.D., Vilinsky, I., Strausfeld, N.J., and Kaiser, K. (1995). Subdivision of the *Drosophila* mushroom bodies by enhancer-trap expression patterns. Neuron *15*, 45–54.